

## Variation in antiviral immunity and inflammation pathways precedes HIV-1 infection in a high-risk African cohort

Mwikali Kioko, Shaban Mwangi, Lynn Fwambah, Amin S. Hassan, Jason T. Blackard, Philip Bejon, Eduard J. Sanders, Thumbi Ndung'u, Eunice W. Nduati, Abdirahman I. Abdi

*J Clin Invest.* 2026. <https://doi.org/10.1172/JCI195172>.

**Clinical Research and Public Health** **In-Press Preview** **AIDS/HIV** **Immunology** **Infectious disease**

**BACKGROUND.** Susceptibility to human immunodeficiency virus type 1 (HIV-1) infection varies between individuals, but the biological determinants of acquisition risk remain poorly defined.

**METHODS.** We conducted a case-control study nested within a high-risk cohort in Kenya. We compared the plasma extracellular RNA collected before HIV-1 acquisition with matched uninfected controls to identify immunological processes linked to infection risk.

**RESULTS.** Individuals who later acquired HIV-1 exhibited upregulation of immune processes that facilitate viral infection, including T cell suppression, type II interferon and Th2 immune responses. In contrast, processes associated with antiviral defence and tissue repair, such as neutrophil and natural killer cell responses, type I interferon responses, wound healing, and angiogenesis, were downregulated.

**CONCLUSION.** These findings highlight dampened antiviral immunity prior to exposure as a correlate of increased risk for subsequent HIV-1 acquisition.

**TRIAL NUMBERS.** Not applicable.

**FUNDING.** This work was supported by a Wellcome Trust Award (209289/Z/17/Z) and the Sub-Saharan African Network for TB/HIV Research Excellence (SANTHE) through the DELTAS Africa programme [Del-22-007], supported by the Science for Africa Foundation, Wellcome Trust, the UK Foreign, Commonwealth & Development Office, and the European Union. Additional support was provided by the Bill & Melinda Gates Foundation, Gilead Sciences Inc., Aidsfonds, and the Ragon Institute of Mass General, MIT, and Harvard. The cohort study was supported by PEPFAR through USAID. The views expressed [...]

**Find the latest version:**

<https://jci.me/195172/pdf>



1 **Variation in antiviral immunity and inflammation pathways**

2 **precedes HIV-1 infection in a high-risk African cohort**

3 Mwikali Kioko<sup>1\*</sup>, Shaban Mwangi<sup>1</sup>, Lynn Fwambah<sup>1</sup>, Amin S. Hassan<sup>1,2</sup>,

4 Jason T. Blackard<sup>3</sup>, Philip Bejon<sup>1,4</sup>, Eduard Sanders<sup>5,6</sup>, Thumbi

5 Ndung'u<sup>7,8,9,10</sup>, Eunice W. Nduati<sup>1,4,11†</sup>, Abdirahman I. Abdi<sup>1,4,11†</sup>

6 <sup>1</sup>Bioscience Department, Kenya Medical Research Institute-Wellcome

7 Trust Research Programme, Kilifi, Kenya

8 <sup>2</sup>Institute for Human Development, Aga Khan University, Nairobi, Kenya

9 <sup>3</sup>Division of Gastroenterology & Hepatology, University of Cincinnati

10 College of Medicine, Cincinnati, Ohio, USA

11 <sup>4</sup>Centre for Tropical Medicine and Global Health, Nuffield Department of

12 Medicine, University of Oxford, Oxford, UK

13 <sup>5</sup>Sir William Dunn School of Pathology, University of Oxford, Oxford, UK

14 <sup>6</sup>The Aurum Institute, Johannesburg, South Africa

15 <sup>7</sup>Africa Health Research Institute, Durban, South Africa

16 <sup>8</sup>HIV Pathogenesis Programme, The Doris Duke Medical Research

17 Institute, University of KwaZulu-Natal, Durban, South Africa

18 <sup>9</sup>Ragon Institute of Mass General Brigham, Massachusetts Institute of  
19 Technology and Harvard University, Cambridge, MA, USA

20 <sup>10</sup>Division of Infection and Immunity, University College London, London,  
21 UK

22 <sup>11</sup>Pwani University Biosciences Research Centre, Pwani University, Kilifi,  
23 Kenya

24 \*To whom correspondence should be addressed: Mwikali Kioko: P.O Box  
25 230-80108, Kilifi, Kenya, +254711776932, [kmwikali@kemri-](mailto:kmwikali@kemri-wellcome.org)  
26 [wellcome.org](http://wellcome.org)

27 †These authors share senior authorship.

28 **Conflict-of-interest**

29 The authors have declared that no conflict of interest exists.

30 **ABSTRACT**

31 **Background**

32 Susceptibility to human immunodeficiency virus type 1 (HIV-1) infection  
33 varies between individuals, but the biological determinants of acquisition  
34 risk remain poorly defined.

35 **Methods**

36 We conducted a case-control study nested within a high-risk cohort in  
37 Kenya. We compared the plasma extracellular RNA collected before  
38 HIV-1 acquisition with matched uninfected controls to identify  
39 immunological processes linked to infection risk.

40 **Results**

41 Individuals who later acquired HIV-1 exhibited upregulation of immune  
42 processes that facilitate viral infection, including T cell suppression, type  
43 II interferon and Th2 immune responses. In contrast, processes  
44 associated with antiviral defence and tissue repair, such as neutrophil  
45 and natural killer cell responses, type I interferon responses, wound  
46 healing, and angiogenesis, were downregulated.

47 **Conclusion**

48 These findings highlight damped antiviral immunity prior to exposure  
49 as a correlate of increased risk for subsequent HIV-1 acquisition.

50 **Trial number**

51 Not applicable

52 **Funding**

53 This work was supported by a Wellcome Trust Award (209289/Z/17/Z)  
54 and the Sub-Saharan African Network for TB/HIV Research Excellence  
55 (SANTHE) through the DELTAS Africa programme [Del-22-007],  
56 supported by the Science for Africa Foundation, Wellcome Trust, the UK  
57 Foreign, Commonwealth & Development Office, and the European  
58 Union. Additional support was provided by the Bill & Melinda Gates  
59 Foundation, Gilead Sciences Inc., Aidsfonds, and the Ragon Institute of  
60 Mass General, MIT, and Harvard. The cohort study was supported by  
61 PEPFAR through USAID. The views expressed are those of the authors.

62

63

64

65

66

67

68

69 **INTRODUCTION**

70 Susceptibility to human immunodeficiency virus 1 (HIV-1) infection  
71 varies significantly across populations and individuals (1-3). For  
72 example, analysis from multiple studies showed that sub-Saharan Africa  
73 has a higher risk of HIV-1 transmission per sexual contact compared to  
74 higher-income regions (1). Although these differences may reflect low  
75 access to antiretroviral drugs in sub-Saharan Africa at the time, intra-  
76 population differences in susceptibility have been documented in a  
77 longitudinal study of high-risk Kenyan adults, in which only 7% were  
78 infected during follow-up despite likely widespread exposure (4). This  
79 variability stems from a diverse range of factors, including behavioural  
80 differences, viral load, characteristics of circulating viruses (including  
81 HIV-1 subtype), and host-related factors such as genetic diversity and  
82 environmental exposures such as sexually transmitted infections (STIs)  
83 that can modulate basal immune status (2, 5, 6). However, the specific  
84 host biological factors and pre-existing pathogens associated with HIV-  
85 1 acquisition are not fully known.

86 Identifying biological determinants of HIV-1 susceptibility is crucial for  
87 developing diagnostic biomarkers and interventions (7, 8). High-  
88 throughput omic techniques, including proteomics and transcriptomics,

89 are increasingly employed to understand host mechanisms predisposing  
90 to HIV-1 infections (4, 9). Transcriptomics offers a sensitive method to  
91 detect subtle differences in gene expression, providing insights into the  
92 host's immune response and immunodulatory pathogens (10).

93 All cells secrete a diverse population of RNA collectively called  
94 extracellular RNAs (exRNAs) into biofluids such as plasma, saliva, and  
95 urine (11, 12). The majority of these exRNAs are secreted within  
96 membrane-bound vesicles called extracellular vesicles (EVs), which  
97 protect them in the harsh extracellular space (11-18). Additionally, the  
98 profiles of circulating exRNAs largely reflect the biological state of the  
99 secreting cells, which provides a more holistic view of systemic biological  
100 processes (19-21) and pathogen signals (22-26) relative to the cellular  
101 RNA obtained from peripheral immune cells. Therefore, analyzing  
102 plasma-derived exRNA from pre-infection samples may provide valuable  
103 immune correlates of HIV-1 acquisition.

104 Here, we highlight transcriptional immune correlates of HIV-1  
105 susceptibility by retrospectively analysing plasma-derived exRNA  
106 collected before HIV-1 infection in a case-control study nested within a  
107 longitudinal cohort of HIV-negative high-risk individuals in coastal Kenya  
108 (27).

109 **RESULTS**

110 **Plasma exRNA highlights immunological pathways associated with**  
111 **HIV-1 acquisition risk**

112 The primary objective of this study was to identify pre-infection  
113 transcriptional correlates of HIV-1 acquisition in high-risk adults. To  
114 achieve this, we took advantage of a long-term longitudinal cohort of  
115 high-risk individuals on the Kenyan coast, for whom the dates of HIV  
116 infection have previously been estimated (4, 27-29) as summarised in  
117 Figure 1 and described in detail in the Methods. We compared plasma-  
118 derived exRNA from individuals who later acquired HIV-1 (cases; n=32),  
119 collected approximately 3±2 months prior to the estimated date of  
120 infection, to that from matched negative controls (n=64) (Figure 1). This  
121 analysis identified 767 genes with differentially increased abundance  
122 and 774 genes with significantly decreased abundance in HIV-1 cases  
123 at a false discovery rate (FDR) of less than 5% (Figure 2A). Next, we  
124 performed principal component analysis (PCA) and supervised heatmap  
125 clustering on the differentially enriched genes and found that the  
126 transcriptional profiles of EVs distinguished controls from the HIV-1  
127 cases (Figure 2B, C). The differentially increased genes included the  
128 endothelial nitric oxide synthase (*NOS3*), angiotensin-converting

129 enzyme 2 (*ACE2*), interleukin 17 and 21 receptors (*IL17RA*, *IL17RD*,  
130 *IL21R*), the viral-sensing Toll-like receptor 7 (*TLR7*), and the inhibitor of  
131 *IRF3*- and NF- $\kappa$ B-dependent antiviral response gene (*ILRUN*) (30)  
132 (Figure 2C). In contrast, the differentially decreased genes featured the  
133 pro-angiogenic factor *VEGFA*, the interferon regulatory factors (*IRF1*,  
134 *IRF3*, *IRF4*, and *IRF5*), and the p53 negative regulator *MDM2* (Figure  
135 2C).

136 Cell enrichment analysis demonstrated that the genes upregulated in  
137 HIV-1 cases 3 $\pm$ 2 months prior to infection belonged to cells such as  
138 eosinophils, plasma B cells, central memory CD8-T cells, plamacytoid  
139 dendritic cells (pDCs), and Th2 cells (Figure 2D). In contrast, the  
140 downregulated genes were enriched for signatures associated with  
141 several cell types, including natural killer (NK) cells, B-memory cells, and  
142 neutrophils (Figure 2D). Next, we performed pathway enrichment  
143 analysis of the 767 genes increased in HIV-1 cases, revealing an  
144 overrepresentation of genes linked to endothelial nitric oxide synthase  
145 (eNOS), IL-17 and IL-10 signalling, suppressive T-cell response, and  
146 apoptosis (Figure 2E). Conversely, the 774 genes decreased in HIV-1  
147 cases belonged to a wide range of biological pathways, including  
148 reparative processes (wound healing and p53-signalling pathway) and

149 pathways related to type-I interferon (IFN), including NFKB activation by  
150 protein kinase R (PKR) and IFN-beta signalling (Figure 2E). These  
151 findings suggest that reduced type I interferon and pro-reparative  
152 immune responses, alongside elevated eNOS, suppressive T cell  
153 response, IL17 and IL10 signalling, are strongly linked to HIV-1  
154 acquisition in high-risk adults.

155 **Plasma exRNA clustering uncovers distinct immunological  
156 endotypes in HIV-1 cases and controls.**

157 There could be heterogeneity in the biological mechanisms that underlie  
158 protection or susceptibility to HIV-1 infection, which is obscured when  
159 comparing the average biological signals between cases and controls.  
160 To reveal intragroup heterogeneity and biological signal, we constructed  
161 a participant similarity network (PSN) using the exRNA dataset  
162 generated from the samples collected  $3\pm2$  months prior to HIV-1  
163 infection. Spectral clustering of the similarity network identified five  
164 endotypes of study participants - named A, B, C, D, and E - of which  
165 endotypes A, B, and C were enriched for controls, while D and E were  
166 enriched for HIV-1 cases (Figures 3A-C). We subsequently performed  
167 differential feature analysis and identified over 4000 genes whose  
168 exRNA profiles differed significantly between the endotypes, surpassing

169 the differential signal observed in the case-control analysis (Figure 3D,  
170 Supplemental Table 1). Pathway enrichment analysis revealed that the  
171 control endotypes were enriched for features associated with pro-  
172 reparative processes (wound healing, TGF-beta/SMAD signalling,  
173 VEGF overexpression and histamine metabolism), T cell function (T cell  
174 CD3, T cytotoxic cell surface, co-stimulatory T cell activation, granzyme-  
175 B pathway and CTLA4 signalling), mitochondrial function (protection  
176 against ROS, Keap1-Nrf2, respiratory electron transport, citric acid  
177 cycle), and type I IFN signalling (IFN Beta signalling pathway, cGAS-  
178 STING-TBK1 pathway, TLR-TRIF pathway, NFKB activation by PKR)  
179 (Figure 3E).

180 The two endotypes composed mainly of HIV-1 cases (Figure 3A-C) were  
181 also enriched for distinct pathways, with genes augmented in endotype  
182 D featuring those linked to eNOS signalling, regulatory T cells, CXCR4  
183 signalling, and FAS-mediated apoptosis (Figure 3E). Finally, endotype E  
184 showed evidence of increased apoptosis, including HIV-1 mediated T  
185 cell apoptosis, TRAIL and DR3 death receptor signalling. Signatures of  
186 B-cell differentiation, IL-7 signalling, and suppressor of cytokine  
187 signalling (SOCS) were also enriched in endotype E (Figure 3E). Our  
188 endotyping analysis revealed more differentially expressed genes, and

189 enrichment analysis compared to case-control analysis, which suggests  
190 that different biological mechanisms could promote or impede HIV-1  
191 infection.

192 **The immunological processes observed at 3±2 months were**  
193 **conserved at 6±2 months prior to HIV-1 infection.**

194 To investigate whether the immune profile observed 1 to 5 months prior  
195 to HIV-1 infection was also evident at earlier time points, we analysed  
196 the transcriptional profiles from 9 individuals who later acquired HIV-1  
197 and 29 matched controls who remained uninfected, using samples  
198 collected 4 to 8 months before the cases became HIV-1 positive. We  
199 found that 2688 genes were significantly increased in HIV-1 cases, while  
200 4521 genes were significantly decreased (Figure 4A, Supplemental  
201 Table 2). Cellular enrichment analysis of the altered genes showed  
202 significant downregulation of genes belonging to natural killer cells (e.g.  
203 *NCAM1*, *FCGR3A*), plasma B-cells (e.g. *CD38*), and pDCs (Figure 4A-  
204 B). When we performed pathway over-representation analysis, we  
205 observed that genes upregulated 6±2 months prior to HIV-1 infection  
206 featured those belonging to type II interferon signalling (e.g. *CXCR3*,  
207 *IFNG*, *IL19*, and *CXCL9*) (Figure 4C). On the other hand, genes  
208 downregulated 6±2 months prior to HIV-1 infection were enriched for

209 type I interferon signalling (e.g. *IRF3*, *IRF9*, *JAK1*, *STAT2*, *STAT5A*,  
210 *IL1B*, *TLR2*, *TLR4*), and VEGFA-VEGFR2 signalling, consistent with the  
211 3±2 months prior to infection timepoint (Figure 4C). These observations  
212 confirm that reduced type 1 interferon-driven innate immunity, together  
213 with an elevated type II interferon state, precedes HIV-1 infection.

214 **The presence of human pegivirus type-1 (HPgV-1) is associated  
215 with HIV-1 acquisition.**

216 We next analyzed the exRNAseq data using a metatranscriptomic  
217 approach to nominate potential pathogens associated with HIV-1  
218 susceptibility. HPgV-1 RNA abundance was significantly higher in HIV-1  
219 cases than controls three months before HIV infection ( $\log_2$ fold-  
220 change>4, FDR<0.05) but not at six months (Figure 5A). Applying more  
221 stringent criteria (>5 reads) to define HPgV1 positivity, rather than  
222 considering any detectable HPgV1 RNA level as positive, we identified  
223 20 HPgV1 positives. HPgV-1 positivity was non-significantly higher  
224 among HIV-1 cases than controls at both three months (28% in cases  
225 versus 17% in controls; OR = 1.89, 95% CI 0.69-5.16, p = 0.29) and at  
226 six months (22% in cases versus 14% in controls; OR = 1.79, 95% CI  
227 0.27-11.86, p = 0.61, indicating a modest enrichment of HPgV1 among  
228 individuals who later acquired HIV-1 (Figure 5B). 14 participants were

229 identified as HPgV-1 positive by conventional PCR, of which only 3 of  
230 them were not detected using NGS. (Figure 5C). Poisson regression  
231 analyses showed that HPgV-1 infection detected by next-generation  
232 sequencing (NGS) and PCR at  $3 \pm 2$  months prior to HIV-1 infection was  
233 significantly associated with HIV-1 acquisition (NGS: RR = 1.99, 95% CI  
234 1.11-3.55; PCR: RR = 2.32, 95% CI 1.32-4.08) (Figure 5D). However,  
235 after adjustment for other sexually transmitted infections, the association  
236 was reduced (NGS: RR = 1.51, 95% CI 0.88-2.61; PCR: RR = 1.66, 95%  
237 CI 0.96-2.87), indicating that HPgV-1 was not an independent predictor  
238 of HIV-1 acquisition. We next compared the endotypes by HPgV1 status,  
239 revealing that individuals clustered in endotype D were more likely to be  
240 HPgV1 positive compared to endotypes A or B (Figure 5E). To assess  
241 the impact of HPgV-1 on transcriptional alterations between HIV-1 cases  
242 and controls, we compared the transcriptional difference between HIV-1  
243 cases and controls, before and after adjusting for HPgV-1 status. We  
244 found a high correlation ( $R=0.97$ ,  $P<0.0001$ ) of the  $\log_2$ fold changes  
245 before and after adjusting for HPgV1 (Figure S1, Supplementary Table  
246 3). Further, 120 and 201 of the upregulated and downregulated genes  
247 between HIV-1 cases and controls, respectively, showed significant  
248 differential abundance between HPgV-1 positive and negative  
249 individuals (Figure S2, Supplementary Table 4). We also compared

250 transcriptional changes between HPgV1-positive and -negative  
251 individuals within both the HIV cases and the control groups and found  
252 overlaps of 37 (3.7%) and 38 (4.8%) upregulated and downregulated  
253 genes, respectively (Figure S3; Supplementary Table 5). Additionally, we  
254 reanalysed previously published transcriptional data from PBMCs that  
255 were either exposed or unexposed to HPgV1 *in vitro*. The reanalysis  
256 revealed only 12 genes (6 upregulated and 6 downregulated) with  
257 concordant expression between exRNA and PBMCs (Figure S4 and  
258 Supplementary Table 6).

259 Finally, we assessed the genetic relatedness of the HPgV-1 genome  
260 sequences from the 3±2 months prior to infection samples relative to  
261 those from other parts of the world. We generated 11 partial HPgV-1  
262 genomes, of which 4 were from the controls and 7 were from the HIV-1  
263 cases. We next performed phylogenetic analysis and found that the  
264 HPgV-1 genomes clustered by geographic origin, with our partial  
265 genomes co-clustering with those from other African countries,  
266 consistent with previous studies(31) (Figure 5F).

267

268

269

270 **DISCUSSION**

271 In this study, we leveraged plasma-derived exRNA to determine pre-  
272 infection immune correlates of HIV-1 acquisition among high-risk adults  
273 in a longitudinal cohort study (27, 29). We highlight key findings, explore  
274 their biological relevance to HIV-1 susceptibility, and offer potential  
275 avenues for future research and intervention. Given that the profiles of  
276 circulating exRNA often mirror molecular activities in the tissues most  
277 affected by a specific condition (32), in this case, the mucosal sites that  
278 serve as primary portals of HIV-1 entry, we also discuss our observations  
279 within the context of mucosal immune regulation.

280 Our differential feature analysis showed that, three months prior to HIV-  
281 1 infection, individuals who later got infected exhibited significant  
282 alterations in exRNA profiles compared to the controls. Notably,  
283 transcripts associated with IL-17 receptor signalling, apoptosis,  
284 regulatory T-cells, and eNOS signalling were upregulated in HIV-1  
285 cases. Higher sexual activity, particularly receptive anal intercourse (33-  
286 35), together with STIs, may promote mucosal damage, immune  
287 activation and apoptosis, events that compromise barrier integrity and  
288 facilitate viral entry. The elevated IL-17 receptor and eNOS signalling,  
289 along with Treg responses, may represent compensatory mechanisms

290 that restore mucosal homeostasis (36-43) but could also be induced by  
291 STIs and anal intercourse (33, 44). However, chronic activation of these  
292 pathways could sustain inflammation and tissue damage. Moreover,  
293 enhanced IL-17 receptor signalling may also drive chemokines that  
294 enhance Th17 cell recruitment at mucosal sites (45), key HIV-1 target  
295 cells (46-48). While Tregs help reduce immune activation, they are also  
296 susceptible to HIV-1 infection (49, 50) and can weaken antiviral  
297 response, collectively enhancing susceptibility to HIV-1 acquisition.

298 A key observation from our study was the downregulation of genes linked  
299 to type I interferon response, accompanied by an upregulation of type II  
300 interferon-associated transcripts in individuals who later acquired HIV-1.  
301 This pattern suggests a reprogramming of the immune landscape toward  
302 a less antiviral (30, 51-57) and more inflammatory state, which may  
303 increase the expression of key HIV-1 entry receptors such as CCR5 (58-  
304 60), thereby increasing susceptibility to HIV-1 infection. The  
305 suppression of type I interferon response may be driven by elevated IL-  
306 17 signalling, given that type I interferon and Th17 responses are known  
307 to act antagonistically (61). Indeed, individuals with a gain-of-function  
308 mutation in type 1 interferon signalling are predisposed to fungal  
309 infection due to impaired Th17 responses (62, 63), while chronic

310 hyperactivation of Th17 responses has been associated with increased  
311 susceptibility to viral infections (45, 64, 65).  
312 Our endotyping analysis identified five distinct endotypes, reflecting  
313 significant heterogeneity in the biological mechanisms at play. Three  
314 endotypes - A, B, and C -predominantly comprising controls, displayed  
315 immune profiles consistent with effective antiviral immunity (66, 67) and  
316 restrained immune activation, characterised by enhanced type I  
317 interferon response, T-cell function, TGF-beta/SMAD signalling, and  
318 oxidative phosphorylation. These features likely contribute to efficient  
319 antiviral defence (57) and maintenance of mucosal health. For example,  
320 increased TGF-beta could confer protection against HIV-1 infection  
321 through maintaining an effective mucosal immune system impervious to  
322 viral entry (68, 69) or inhibiting the pro-HIV type II IFN immune response  
323 (70). In contrast, the two susceptibility endotypes, D and E, were  
324 enriched for regulatory T-cells and FAS-mediated signalling, TRAIL, and  
325 SOC3 pathways, signatures that suppress antiviral immunity and  
326 enhance mucosal disruption (71-73). Together, these findings suggest  
327 that pre-infection immune heterogeneity, particularly involving interferon  
328 balance and T-cell function interplay, critically shapes HIV-1 acquisition

329 risk and may inform precision prevention strategies. However, a larger  
330 study is necessary to identify the true heterogeneity of HIV-1 risk.

331 Our metatranscriptomic analysis identified HPgV-1 (also called human  
332 pegivirus C type 1 or GB virus C [GBV-C] or *Pegivirus hominis*) as  
333 significantly associated with HIV-1 acquisition, albeit less pronounced  
334 when adjusting for other STIs. HPgV-1 is a flavivirus that infects  
335 lymphocytes and NK cells and is transmitted by blood transfusion,  
336 sexual exposure, and mother-to-fetal transmission (74). While our data  
337 suggests that HPgV-1 is a correlate of HIV-1 acquisition, its predictive  
338 value is influenced by the presence of other STIs. This suggests that  
339 HPgV-1 may not directly drive susceptibility but instead reflects a  
340 permissive host immune environment conducive to sexually transmitted  
341 viral infection, thus representing a biomarker for HIV-1 risk.

342 Interestingly, during established HIV-1 infection, HPgV-1 has been linked  
343 to slower progression to acute immunodeficiency syndrome (AIDS) (75-  
344 79). A plausible explanation, which is consistent with our data, is that  
345 HPgV-1 exploits an immune milieu characterised by reduced type I and  
346 elevated type II interferon response (80), an immune balance that  
347 favours viral acquisition but limits immunopathology (81-84). However,

348 a direct role for HPgV-1 in modulating host immunity cannot be ruled out,  
349 as suggested by other studies (26, 85-87).

350 The retrospective design of our study represents a key limitation.  
351 Concurrent collection of mucosal samples alongside blood would have  
352 allowed direct validation of the immunological signatures inferred from  
353 exRNA analyses against local mucosal responses. Consequently, some  
354 of our interpretations, although supported by existing literature, remain  
355 speculative and require confirmation through prospective studies.

356 In summary, we highlight the strength of plasma exRNAseq in  
357 uncovering pre-infection biological correlates of HIV-1 acquisition.  
358 Future research should focus on validating the predictive value of HPgV-  
359 1 in larger cohorts and exploring its utility in predictive models and  
360 targeted interventions. In conclusion, understanding the biological  
361 drivers of HIV-1 susceptibility among high-risk populations could  
362 enhance the development of prevention and treatment strategies.

363

364

365

366

367 **METHODS**

368 **Sex as a biological variable**

369 Samples from cases and controls were obtained from both men and  
370 women. In our study, sex was not considered a biological variable of  
371 interest.

372 **Study design and population**

373 *3±2 months prior to HIV-infection samples:* A case-control study nested  
374 in a historic HIV-1 high-risk cohort from Coastal Kenya was conducted.  
375 HIV-1 negative high-risk volunteers, including men-who-have-sex-with-  
376 men (MSM) and female sex workers (FSW) aged  $\geq 18$  years, were  
377 recruited and followed from 2006 to 2011 for HIV-1 vaccine  
378 preparedness studies. Volunteers were screened for incident HIV-1  
379 infection during follow-up using RT-PCR, p24 antigen, and HIV-1-  
380 specific antibody assays as previously described (4, 28). For any  
381 volunteer testing HIV-1 positive, an estimated date of infection (EDI) was  
382 calculated either to be: 10 days before a positive HIV-1 RNA test (if  
383 antibody negative), 14 days before a p24 antigen positive test (if RNA  
384 test was missing), or midway between the last negative and first positive  
385 HIV-1 specific antibody test (if both RNA and p24 tests were missing).  
386 Cases were defined as volunteers who tested HIV-1 positive, while

387 controls were those who remained negative at the end of a similar follow-  
388 up period (4). Plasma samples from cases were collected 3±2 months  
389 prior to the EDI, with controls matched 2:1 to cases based on sex, age,  
390 risk group, follow-up duration, and plasma sample availability.

391 *6±2 months prior to HIV infection samples:* Plasma samples collected  
392 6±2 months before the EDI were retrieved. Controls were matched 2:1  
393 to HIV cases based on age, sex, risk group, follow-up duration in the  
394 study and the availability of plasma samples collected at around the  
395 same calendar date as that of the index case ±2 months.

### 396 **Isolation of extracellular RNA**

397 Nanofiltration and ultracentrifugation were used to isolate exRNA,  
398 aiming to primarily enrich for those encapsulated in small EVs, as  
399 described previously (19). In brief, 13.5 ml of prefiltered PBS was  
400 combined with 300 µL of plasma in a 15 ml Falcon tube. The diluted  
401 plasma was filtered through a 0.22 µm (Millipore) filter to exclude cell  
402 debris and centrifuged at 150,000 x g for 2 hours at 4 °C without  
403 breaks. The pellets were treated with RNase A for 15 min and washed  
404 at 150,000 x g for two hours at 4°C. The impact of the RNase treatment  
405 was evaluated by comparing the exRNA profile before and after  
406 treatment using bioanalyzer/Agilent TapeStation (Figure S5). The

407 supernatant was discarded while the pellets were digested using 250  $\mu$ l  
408 of RNA lysis solution (Bioline) and stored at -80°C until needed. ExRNA  
409 was extracted from the lysed pellets using the Isolate II RNA Mini Kit  
410 (Bioline) as directed by the manufacturer.

411 **Bead-assisted flow cytometry**

412 Evaluation of small EV markers in our pellets was performed using bead-  
413 assisted flow cytometry (Figure S5), as we previously described (88).  
414 Briefly, 50  $\mu$ L of EVs in PBS were incubated with 1  $\mu$ L of aldehyde/sulfate  
415 latex beads (Invitrogen) in a total volume of 1 mL PBS for 12 hours at  
416 room temperature on a rotary mixer. Following incubation, 110  $\mu$ L of 1 M  
417 glycine was added to block unreacted sites, and the mixture was  
418 incubated for an additional 30 minutes at room temperature. Beads were  
419 pelleted by centrifugation at 2000  $\times g$  for 5 minutes and washed once  
420 with 1 mL PBS. The pellet was resuspended in PBS supplemented with  
421 0.5% fetal bovine serum (PBS + 0.5% FBS) and stained with 1 $\times$  anti-  
422 CD9-APC (Cat. No. 341648, BD Biosciences) and 1 $\times$  anti-CD63-PE  
423 (Cat. No. 55705, BD Biosciences). Negative controls included beads  
424 incubated with (i) antibody cocktail without EVs, and (ii) isotype control  
425 antibodies: PE mouse IgG1 (Cat. No. 556650, BD Biosciences) and APC  
426 mouse IgG1 (Cat. No. 550854, BD Biosciences). Stained beads were

427 washed twice with 500  $\mu$ L PBS + 0.5% FBS and pelleted by  
428 centrifugation at 2000  $\times g$  for 10 minutes. Data acquisition was  
429 performed using a BD Fortessa flow cytometer.

430 **cDNA library preparation**

431 We used our previous protocol(19, 88) to prepare the cDNA libraries for  
432 sequencing. Briefly, Superscript III (Invitrogen) was used to produce the  
433 first strand from the total exRNA. Before synthesizing the second strand,  
434 the first strand reaction was cleaned using RNACleanXP beads. dTTP  
435 was replaced with dUTP while synthesizing the second strand to  
436 generate double-stranded cDNA. The cDNA was fragmented, end-  
437 repaired and ligated to adapters. The cDNA was treated with USER  
438 followed by 19 cycles of PCR amplification to add Illumina primers and  
439 increase yield. Sequencing was performed using the NextSeq 550  
440 genome analyzer.

441 **Quantification of HPgV-1 using PCR**

442 HPgV-1 RNA was converted to cDNA using Superscript III reverse  
443 transcriptase (NEB). HPgV-1 positive samples were detected by  
444 amplicon-targeted PCR amplification of the 5' untranslated region (UTR)  
445 with the antisense primer 5' - ATG CCA CCC GCC CTC ACC CGAA -  
446 3' (nucleotides [nt] 494-473 according to GenBank accession number

447 AY196904) and the sense primer 5' - AAA GGT GGT GGA TGG GTG  
448 ATG - 3' (nt 67-87) using Q5® High-Fidelity DNA Polymerase (New  
449 England Biolabs). Amplification conditions were 50°C for 59 minutes, 10  
450 minutes at 94°C, then 35 cycles of 30 seconds at 94°C, 1 minute at 55°C,  
451 and 1 minute at 72°C, followed by 20 minutes at 72°C. First-round  
452 polymerase chain reaction (PCR) products were used in nested PCR  
453 with the antisense primer 5' – CCC CAC TGG TCY TTG YCA ACT C -  
454 3' (nt 362-341) and sense primer 5' – AAT CCC GGT CAY AYT GGT  
455 AGC CAC T - 3' (nt 107-131). After 35 cycles of 30 seconds at 94°C, 30  
456 seconds at 55°C, and 1 minute at 72°C, PCR products were visualized  
457 by agarose gel electrophoresis for the presence of a 256 nt band.

#### 458 **Statistics**

459 Gene body read coverage depicted in Figure S7 was calculated using  
460 the *RSEQC* tool. Transcript quantities in the units of raw read counts and  
461 transcripts per million (TPM) were estimated by aligning the data to the  
462 human transcriptomes using *salmon* and *tximport*. Comparison between  
463 cases and controls was performed using *edgeR*. Raw read counts were  
464 normalized using the relative log expression (RLE) method, and the  
465 likelihood ratio test was chosen. *P*-values were adjusted for multiple  
466 testing using the Benjamini-Hochberg statistical procedure, and an FDR

467 threshold of less than 5% was set as the cut-off for significance.  
468 Endotyping was conducted using spectral clustering, while differences  
469 in gene expression between the endotypes were determined in *edgeR*  
470 as described above. Cellular overrepresentation was performed using  
471 protein signatures derived from a previously published study(89) while  
472 pathway genesets were obtained from *Literature Lab*(90) and  
473 *Wikipathway*(91). Pathogen classification was performed using Kraken2,  
474 while a comparison of pathogen abundance between cases and controls  
475 was performed using *edgeR*. In parallel, the predictive value of HPgV-1,  
476 as measured by both sequencing and PCR, was also assessed by  
477 calculating risk ratios, with or without adjustment of other STIs. HPgV-1  
478 phylogenetic tree was generated by first performing multiple sequence  
479 alignment using *nextalign* followed by tree reconstruction using *iqtree*.  
480 Unless stated otherwise, all visualizations were carried out using *ggplot2*  
481 and *ComplexHeatmap* R packages.

482

483

484

485

486 **STUDY APPROVAL**

487 The samples used in this study were collected using the IAVI protocol B,  
488 reviewed by the Kenya Medical Research Institute Ethical Review  
489 Committee. Participants provided their written informed consent.

490 **DATA AVAILABILITY**

491 This study did not produce unique reagents or materials. RNAseq data  
492 have been deposited at GEO under the accession number GSE287060  
493 (<https://www.ncbi.nlm.nih.gov/geo/query/acc.cgi?acc=GSE287060>).  
494 Datapoint values for all graphs are available in the Supporting Data  
495 Values file.

496 **AUTHOR CONTRIBUTIONS**

497 A.I.A. E.W.N. and T.N. jointly conceived the project and secured funding.  
498 P.B. guided data analysis and review of the manuscript. E.S. designed  
499 and ran the cohort and contributed to the study design and review of the  
500 manuscript. L.F. and A.S.H. participated in the study design and sample  
501 selection. M.K. and S.M. performed the laboratory experiments. M.K.  
502 performed data analysis and wrote the initial draft. J.B. designed HPgV-  
503 1 primers and assisted in project conception. A.I.A. and E.W.N. jointly  
504 supervised the project. All authors read and reviewed the final draft.

505 **ACKNOWLEDGEMENT**

506 This research was supported by a Wellcome Trust Award (209289/Z/17/Z) and  
507 the Sub-Saharan African Network for TB/HIV Research Excellence (SANTHE)  
508 which is administered by the Africa Health Research Institute (AHRI) and funded  
509 by the Science for Africa Foundation to the Developing Excellence in  
510 Leadership, Training and Science in Africa (DELTAS Africa) programme [Del-  
511 22-007] with support from Wellcome Trust and the UK Foreign, Commonwealth  
512 & Development Office and is part of the EDCPT2 programme supported by the  
513 European Union; the Bill & Melinda Gates Foundation [INV-033558]; Gilead  
514 Sciences Inc., [19275], Aidsfonds [0454] and the Ragon Institute of Mass  
515 General, MIT, and Harvard. The cohort study was conducted by IAVI with  
516 support of the American People through the U.S. President's Emergency Plan  
517 for AIDS Relief (PEPFAR) through United States Agency for International  
518 Development (USAID). All content contained within is that of the authors and  
519 does not necessarily reflect the positions or policies of the funders. For the  
520 purpose of open access, the author has applied a CC BY public copyright  
521 licence to any Author Accepted Manuscript version arising from this submission.  
522 This manuscript is published with permission of the Director, KEMRI.

523

524

525

526 **SUPPLEMENTAL TABLES**

527 Supplemental Table 1: excel file containing additional data related to  
528 Figure 3.

529 Supplemental Table 2: excel file containing additional data related to  
530 Figure 4.

531 Supplemental Table 3: excel file containing additional data related to  
532 Figures S1

533 Supplemental Table 4: excel file containing additional data related to  
534 Figures S2

535 Supplemental Table 5: excel file containing additional data related to  
536 Figures S3

537 Supplemental Table 6: excel file containing additional data related to  
538 Figures S4

539

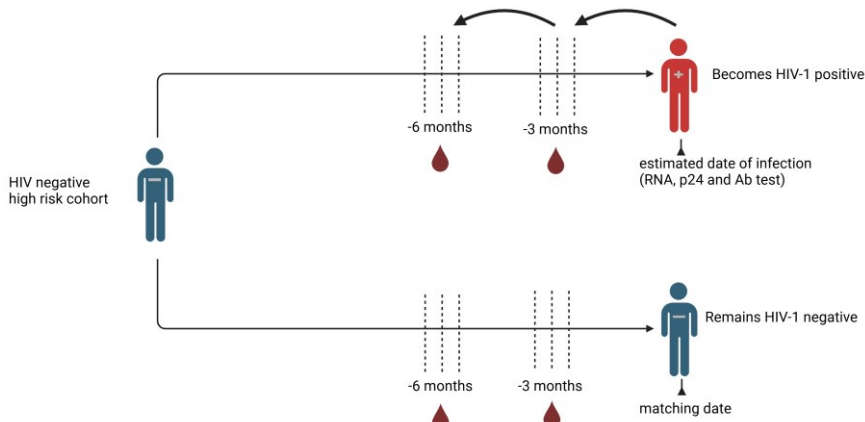
540

541

542

543

## Figure and legends



544

545

**Figure 1: Schematic representation of our study design.** Three and six-month prior to HIV infection, samples were selected from a historic high-risk cohort study conducted on the Kenyan coast between 2006 and 2011. Cases were defined as those who tested HIV positive during follow-up using RT-PCR, p24 antigen, and HIV-1-specific antibody assays. Controls were those who remained HIV-negative during follow-up and were matched to the cases based on sex, age, risk group, follow-up duration, and availability of samples.

546

547

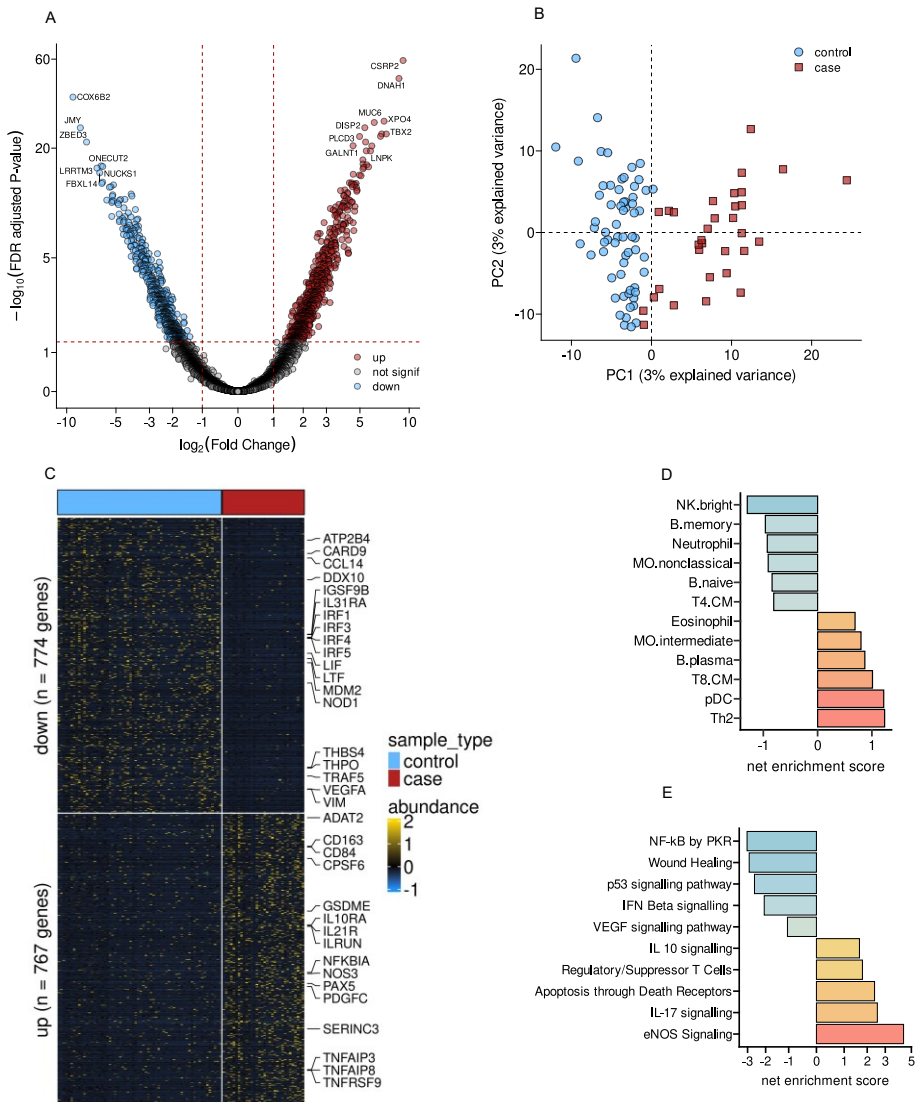
548

549

550

551

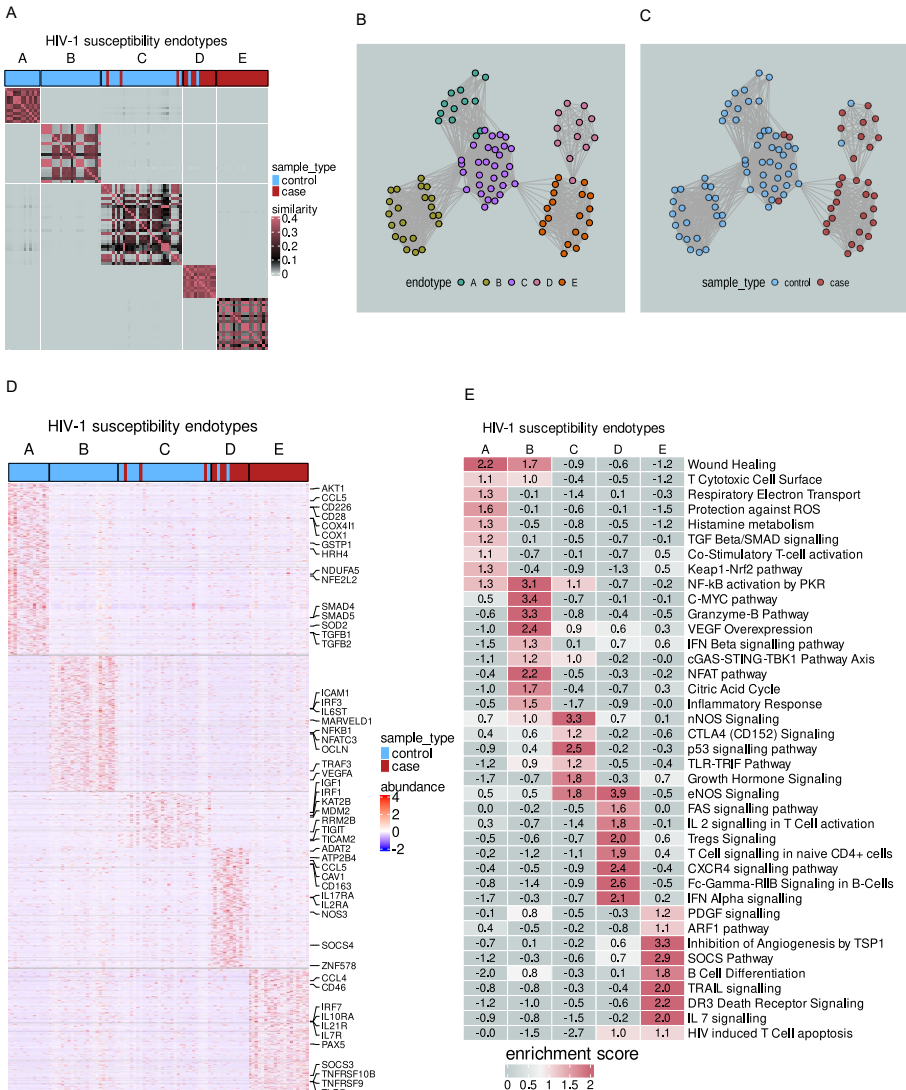
552



553

554 **Figure 2: Cases exhibited a deregulated immunological profile**  
 555 **three months prior to HIV-1 infection**

556 (A) Volcano plot showing differentially altered genes between 32 cases  
557 and 64 controls, three months prior to cases being HIV positive. Red  
558 dots represent genes upregulated in cases, blue represents  
559 downregulated genes, and grey represents unaltered genes. (B) The  
560 differentially altered genes can distinguish HIV-1 cases from those who  
561 remained negative. (C) Supervised heatmap clustering showing  
562 differences in gene expression between cases and controls. (D) Gene  
563 enrichment analysis showing transcriptional alteration at the cellular  
564 level. Genes belonging to neutrophils were downregulated, while those  
565 belonging to eosinophils and memory Tregs (mTregs) were upregulated.  
566 (E) Pathway gene enrichment analysis shows that immunosuppressive  
567 biological processes, such as IL10 signalling and regulatory T cells, were  
568 upregulated in the cases, while inflammatory and reparative processes  
569 were downregulated.



570

571 **Figure 3: Cases and controls cluster into distinct immunological**  
 572 **endotypes three months prior to HIV-1 infection**

573 (A) Patient similarity matrix showing that EVs-RNAseq data, three  
574 months prior to HIV-1 infection, splits controls and cases into three and  
575 two endotypes, respectively. (B and C) Patient similarity network colored  
576 by (B) endotype and (C) sample type. Each node represents a study  
577 participant, and each edge links two similar samples. (D) Heatmap  
578 clustering shows that the identified endotypes have distinct  
579 transcriptional profiles. (E) Heatmap showing the top pathways enriched  
580 in each endotype.

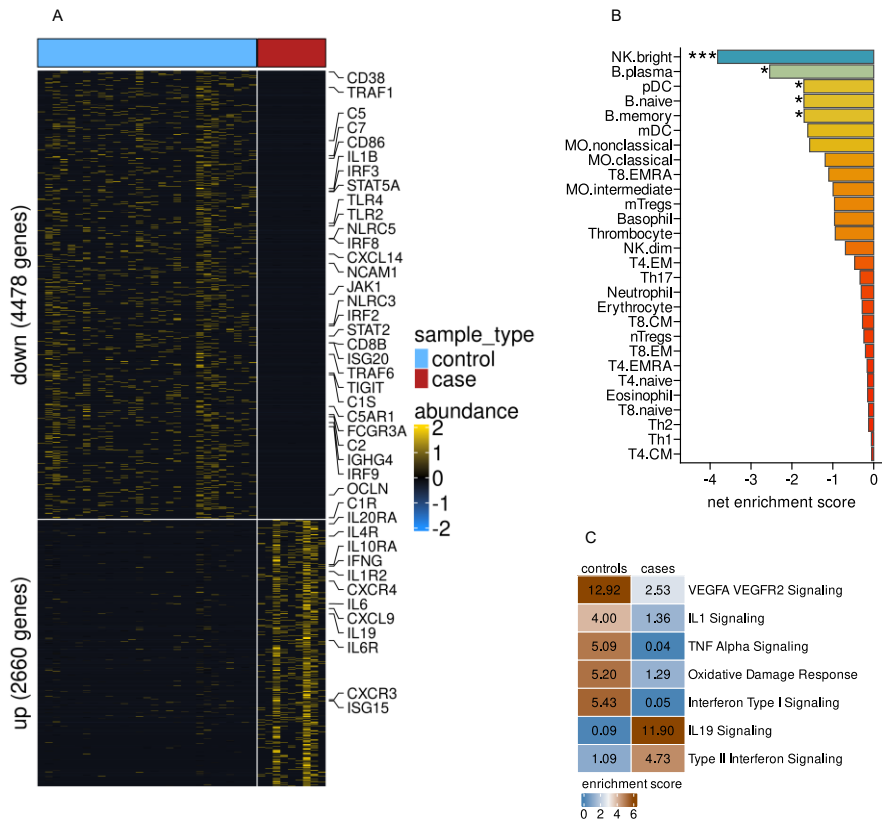
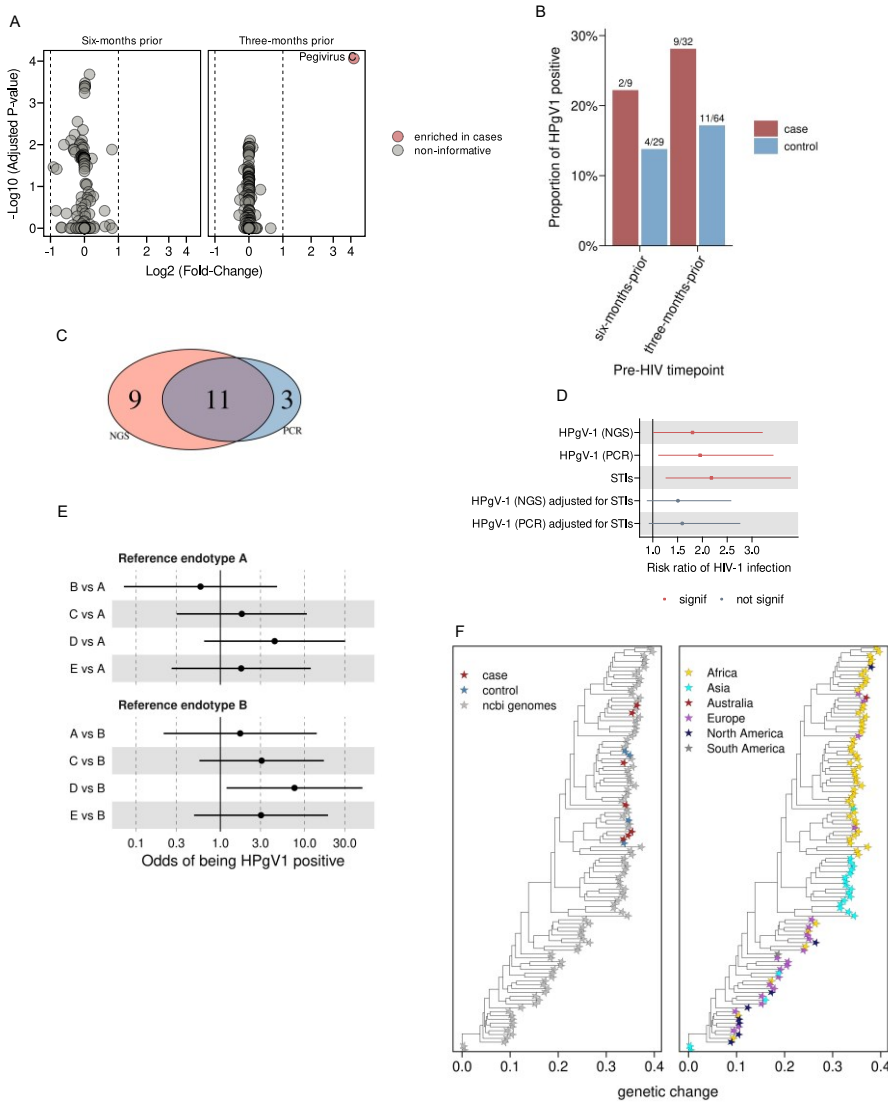


**Figure 4: The immunosuppressive transcriptional profile is also evident six months prior to HIV-1 infection.**

(A) Heatmap showing differential gene expression between 9 cases and 29 controls six months prior to HIV-1 infection. (B) Genes belonging to NK cells and plasma B-cell subsets are severely downregulated in HIV-1 cases relative to controls six months prior to infection. (C) Type II interferon response is upregulated in HIV-1 cases six months prior to infection, while type I interferon response pathways are upregulated.



590

591 **Figure 5: HPgV-1 infection predicts HIV-1 acquisition.**

592 (A) HPgV-1 RNA is more abundant in cases compared to controls at six  
 593 months prior to HIV-1 infection, but not at six months. (B) Barplots

594 showing the proportion of HPgV1 positive in HIV1 cases and controls.  
595 (C) Venndiagram showing overlap of HPgV-1 detection using next-  
596 generation sequencing (NGS) and conventional PCR. (D) The presence  
597 of HPgV-1 three months prior to infection is a non-independent predictor  
598 of HIV-1 infection. (E) Forest plots comparing HPgV1 status between the  
599 endotypes described in Figure 2. (F) HPgV-1 genomes exhibit regional  
600 clustering.

601

1. Boily MC, Baggaley RF, Wang L, Masse B, White RG, Hayes RJ, et al. Heterosexual risk of HIV-1 infection per sexual act: systematic review and meta-analysis of observational studies. *Lancet Infect Dis.* 2009;9(2):118-29.
2. Lama J, and Planelles V. Host factors influencing susceptibility to HIV infection and AIDS progression. *Retrovirology.* 2007;4:52.
3. Marmor M, Hertzmark K, Thomas SM, Halkitis PN, and Vogler M. Resistance to HIV infection. *J Urban Health.* 2006;83(1):5-17.
4. Fwambah L, Andisi C, Streatfield C, Bromell R, Hare J, Esbjörnsson J, et al. Exposure to common infections may shape basal immunity and potentially HIV-1 acquisition amongst a high-risk population in Coastal Kenya. *Front Immunol.* 2023;14:1283559.
5. Nigat AB, Abate MW, Demelash AT, Bantie B, Tibebu NS, Tiruneh CM, et al. Predictors of HIV/AIDS preventive behavior among undergraduate health science university students in Northwest Ethiopia, 2022. Institution-based cross-sectional study. *Helijon.* 2024;10(11):e32453.
6. Santos Í M, da Rosa EA, Gräf T, Ferreira LG, Petry A, Cavalheiro F, et al. Analysis of Immunological, Viral, Genetic, and Environmental Factors That Might Be Associated with Decreased Susceptibility to HIV Infection in Serodiscordant Couples in Florianópolis, Southern Brazil. *AIDS Res Hum Retroviruses.* 2015;31(11):1116-25.
7. Hulse SV, Antonovics J, Hood ME, and Bruns EL. Host-pathogen coevolution promotes the evolution of general, broad-spectrum resistance and reduces foreign pathogen spillover risk. *Evol Lett.* 2023;7(6):467-77.
8. Pirrone V, Mell J, Janto B, and Wigdahl B. Biomarkers of HIV Susceptibility and Disease Progression. *EBioMedicine.* 2014;1(2-3):99-100.
9. Grabowska K, Harwood E, and Ciborowski P. HIV and Proteomics: What We Have Learned from High Throughput Studies. *Proteomics Clin Appl.* 2021;15(1):e2000040.

635 10. Musimbi ZD, Rono MK, Otieno JR, Kibinge N, Ochola-Oyier LI, de  
636 Villiers EP, et al. Peripheral blood mononuclear cell transcriptomes  
637 reveal an over-representation of down-regulated genes associated  
638 with immunity in HIV-exposed uninfected infants. *Sci Rep.*  
639 2019;9(1):18124.

640 11. Akat KM, Lee YA, Hurley A, Morozov P, Max KE, Brown M, et al.  
641 Detection of circulating extracellular mRNAs by modified small-  
642 RNA-sequencing analysis. *JCI Insight.* 2019;5(9).

643 12. Ji J, Chen R, Zhao L, Xu Y, Cao Z, Xu H, et al. Circulating exosomal  
644 mRNA profiling identifies novel signatures for the detection of  
645 prostate cancer. *Molecular Cancer.* 2021;20(1):58.

646 13. Tamura T, Yoshioka Y, Sakamoto S, Ichikawa T, and Ochiya T.  
647 Extracellular vesicles as a promising biomarker resource in liquid  
648 biopsy for cancer. *Extracellular Vesicles and Circulating Nucleic  
649 Acids.* 2021;2(2):148.

650 14. Arroyo JD, Chevillet JR, Kroh EM, Ruf IK, Pritchard CC, Gibson DF, et  
651 al. Argonaute2 complexes carry a population of circulating  
652 microRNAs independent of vesicles in human plasma. *Proc Natl  
653 Acad Sci U S A.* 2011;108(12):5003-8.

654 15. Turchinovich A, Weiz L, Langheinz A, and Burwinkel B.  
655 Characterization of extracellular circulating microRNA. *Nucleic  
656 Acids Res.* 2011;39(16):7223-33.

657 16. O'Grady T, Njock M-S, Lion M, Bruyr J, Mariavelle E, Galvan B, et al.  
658 Sorting and packaging of RNA into extracellular vesicles shape  
659 intracellular transcript levels. *BMC Biology.* 2022;20(1):72.

660 17. Payandeh Z, Tangruksa B, Synnergren J, Heydarkhan-Hagvall S,  
661 Nordin JZ, Andaloussi SE, et al. Extracellular vesicles transport RNA  
662 between cells: Unraveling their dual role in diagnostics and  
663 therapeutics. *Mol Aspects Med.* 2024;99:101302.

664 18. Leidal AM, Huang HH, Marsh T, Solvik T, Zhang D, Ye J, et al. The  
665 LC3-conjugation machinery specifies the loading of RNA-binding  
666 proteins into extracellular vesicles. *Nat Cell Biol.* 2020;22(2):187-  
667 99.

668 19. Kioko M, Mwangi S, Pance A, Ochola-Oyier LI, Kariuki S, Newton C,  
669 et al. The mRNA content of plasma extracellular vesicles provides  
670 a window into molecular processes in the brain during cerebral  
671 malaria. *Science Advances*. 2024;10(33):eadl2256.

672 20. Yin H, Xie J, Xing S, Lu X, Yu Y, Ren Y, et al. Machine learning-based  
673 analysis identifies and validates serum exosomal proteomic  
674 signatures for the diagnosis of colorectal cancer. *Cell Reports  
675 Medicine*. 2024;5(8).

676 21. Xu F, Wang K, Zhu C, Fan L, Zhu Y, Wang JF, et al. Tumor-derived  
677 extracellular vesicles as a biomarker for breast cancer diagnosis  
678 and metastasis monitoring. *iScience*. 2024;27(4).

679 22. DeMarino C, Denniss J, Cowen M, Norato G, Dietrich DK,  
680 Henderson L, et al. HIV-1 RNA in extracellular vesicles is associated  
681 with neurocognitive outcomes. *Nature Communications*.  
682 2024;15(1):4391.

683 23. Gould SJ, Booth AM, and Hildreth JE. The Trojan exosome  
684 hypothesis. *Proc Natl Acad Sci U S A*. 2003;100(19):10592-7.

685 24. Lenassi M, Cagney G, Liao M, Vaupotic T, Bartholomeeusen K,  
686 Cheng Y, et al. HIV Nef is secreted in exosomes and triggers  
687 apoptosis in bystander CD4+ T cells. *Traffic*. 2010;11(1):110-22.

688 25. Uemura T, Kawashima A, Jingushi K, Motooka D, Saito T, Nesrine S,  
689 et al. Bacteria-derived DNA in serum extracellular vesicles are  
690 biomarkers for renal cell carcinoma. *Helijon*. 2023;9(9).

691 26. Stapleton JT, Xiang J, McLinden JH, Bhattacharai N, Chivero ET,  
692 Klinzman D, et al. A novel T cell evasion mechanism in persistent  
693 RNA virus infection. *Trans Am Clin Climatol Assoc*. 2014;125:14-  
694 24; discussion -6.

695 27. Price MA, Kilembe W, Ruzagira E, Karita E, Inambao M, Sanders EJ,  
696 et al. Cohort Profile: IAVI's HIV epidemiology and early infection  
697 cohort studies in Africa to support vaccine discovery. *Int J  
698 Epidemiol*. 2021;50(1):29-30.

699 28. Hassan AS, Pybus OG, Sanders EJ, Albert J, and Esbjörnsson J.  
700 Defining HIV-1 transmission clusters based on sequence data.  
701 *Aids*. 2017;31(9):1211-22.

702 29. Kamali A, Price MA, Lakhi S, Karita E, Inambao M, Sanders EJ, et al.  
703 Creating an African HIV clinical research and prevention trials  
704 network: HIV prevalence, incidence and transmission. *PLoS One*.  
705 2015;10(1):e0116100.

706 30. Trbolet L, Brice AM, Fulford TS, Layton DS, Godfrey DI, Bean AGD,  
707 et al. Identification of a novel role for the immunomodulator ILRUN  
708 in the development of several T cell subsets in mice.  
709 *Immunobiology*. 2023;228(3):152380.

710 31. Samadi M, Salimi V, Haghshenas MR, Miri SM, Mohebbi SR, and  
711 Ghaemi A. Clinical and molecular aspects of human pegiviruses in  
712 the interaction host and infectious agent. *Virology Journal*.  
713 2022;19(1):41.

714 32. Kioko M, Mwangi S, Pance A, Ochola-Oyier LI, Kariuki S, Newton C,  
715 et al. The mRNA content of plasma extracellular vesicles provides  
716 a window into molecular processes in the brain during cerebral  
717 malaria. *Sci Adv*. 2024;10(33):eadl2256.

718 33. Kelley CF, Kraft CS, de Man TJ, Duphare C, Lee HW, Yang J, et al. The  
719 rectal mucosa and condomless receptive anal intercourse in HIV-  
720 negative MSM: implications for HIV transmission and prevention.  
721 *Mucosal immunology*. 2017;10(4):996-1007.

722 34. Kelley CF, Pollack I, Yacoub R, Zhu Z, Van Doren VE, Gumber S, et  
723 al. Condomless receptive anal intercourse is associated with  
724 markers of mucosal inflammation in a cohort of men who have sex  
725 with men in Atlanta, Georgia. *J Int AIDS Soc*. 2021;24(12):e25859.

726 35. Van Doren VE, Ackerley CG, Arthur RA, Murray PM, Smith SA, Hu YJ,  
727 et al. Rectal mucosal inflammation, microbiome, and wound  
728 healing in men who have sex with men who engage in receptive  
729 anal intercourse. *Sci Rep*. 2024;14(1):31598.

730 36. Wacleche VS, Landay A, Routy J-P, and Ancuta P. The Th17 Lineage:  
731 From Barrier Surfaces Homeostasis to Autoimmunity, Cancer, and  
732 HIV-1 Pathogenesis. *Viruses*. 2017;9(10):303.

733 37. Matsushita K, Morrell CN, Cambien B, Yang SX, Yamakuchi M, Bao  
734 C, et al. Nitric oxide regulates exocytosis by S-nitrosylation of N-  
735 ethylmaleimide-sensitive factor. *Cell*. 2003;115(2):139-50.

736 38. Yazji I, Sodhi CP, Lee EK, Good M, Egan CE, Afrazi A, et al.  
737 Endothelial TLR4 activation impairs intestinal microcirculatory  
738 perfusion in necrotizing enterocolitis via eNOS-NO-nitrite  
739 signaling. *Proc Natl Acad Sci U S A.* 2013;110(23):9451-6.

740 39. Good M, Sodhi CP, Yamaguchi Y, Jia H, Lu P, Fulton WB, et al. The  
741 human milk oligosaccharide 2'-fucosyllactose attenuates the  
742 severity of experimental necrotising enterocolitis by enhancing  
743 mesenteric perfusion in the neonatal intestine. *Br J Nutr.*  
744 2016;116(7):1175-87.

745 40. Shang Q, Bao L, Guo H, Hao F, Luo Q, Chen J, et al. Contribution of  
746 glutaredoxin-1 to S-glutathionylation of endothelial nitric oxide  
747 synthase for mesenteric nitric oxide generation in experimental  
748 necrotizing enterocolitis. *Transl Res.* 2017;188:92-105.

749 41. Hosfield BD, Hunter CE, Li H, Drucker NA, Pecoraro AR, Manohar  
750 K, et al. A hydrogen-sulfide derivative of mesalamine reduces the  
751 severity of intestinal and lung injury in necrotizing enterocolitis  
752 through endothelial nitric oxide synthase. *Am J Physiol Regul Integr  
753 Comp Physiol.* 2022;323(4):R422-r31.

754 42. Zhang X, Tian B, Deng Q, Cao J, Ding X, Liu Q, et al. Nicotinamide  
755 riboside relieves the severity of experimental necrotizing  
756 enterocolitis by regulating endothelial function via eNOS  
757 deacetylation. *Free Radic Biol Med.* 2022;184:218-29.

758 43. Li X, Bechara R, Zhao J, McGeachy MJ, and Gaffen SL. IL-17  
759 receptor-based signaling and implications for disease. *Nat  
760 Immunol.* 2019;20(12):1594-602.

761 44. Chao YY, Puhach A, Frieser D, Arunkumar M, Lehner L, Seeholzer T,  
762 et al. Human T(H)17 cells engage gasdermin E pores to release IL-  
763 1 $\alpha$  on NLRP3 inflammasome activation. *Nat Immunol.*  
764 2023;24(2):295-308.

765 45. Wiche Salinas TR, Gosselin A, Raymond Marchand L, Moreira  
766 Gabriel E, Tastet O, Goulet JP, et al. IL-17A reprograms intestinal  
767 epithelial cells to facilitate HIV-1 replication and outgrowth in CD4+  
768 T cells. *iScience.* 2021;24(11):103225.

769 46. Stieh DJ, Matias E, Xu H, Fought AJ, Blanchard JL, Marx PA, et al.  
770 Th17 Cells Are Preferentially Infected Very Early after Vaginal



806 TLR7-Mediated Type I IFN Production of Human Plasmacytoid  
807 Dendritic Cells. *J Immunol.* 2018;200(12):4024-35.

808 55. Kent SJ, and Kelleher AD. Expanding role for type I Interferons in  
809 restricting HIV growth. *Immunol Cell Biol.* 2017;95(5):417-8.

810 56. Goodbourn S, Didcock L, and Randall RE. Interferons: cell  
811 signalling, immune modulation, antiviral response and virus  
812 countermeasures. *J Gen Virol.* 2000;81(Pt 10):2341-64.

813 57. Veazey RS, Pilch-Cooper HA, Hope TJ, Alter G, Carias AM, Sips M,  
814 et al. Prevention of SHIV transmission by topical IFN- $\beta$  treatment.  
815 *Mucosal Immunol.* 2016;9(6):1528-36.

816 58. Roff SR, Noon-Song EN, and Yamamoto JK. The Significance of  
817 Interferon- $\gamma$  in HIV-1 Pathogenesis, Therapy, and Prophylaxis. *Front*  
818 *Immunol.* 2014;4:498.

819 59. Zella D, Barabitskaja O, Burns JM, Romerio F, Dunn DE, Revello MG,  
820 et al. Interferon-gamma increases expression of chemokine  
821 receptors CCR1, CCR3, and CCR5, but not CXCR4 in moncytoid  
822 U937 cells. *Blood.* 1998;91(12):4444-50.

823 60. Liptrott NJ, Egan D, Back DJ, and Owen A. IFN- $\gamma$  874A>T genotype is  
824 associated with higher CCR5 expression in peripheral blood  
825 mononuclear cells from HIV+ patients. *J Acquir Immune Defic*  
826 *Syndr.* 2011;58(5):442-5.

827 61. Zhang W, Chen X, Gao G, Xing S, Zhou L, Tang X, et al. Clinical  
828 Relevance of Gain- and Loss-of-Function Germline Mutations in  
829 STAT1: A Systematic Review. *Front Immunol.* 2021;12:654406.

830 62. Erdős M, Jakobicz E, Soltész B, Tóth B, Bata-Csörgő Z, and Maródi  
831 L. Recurrent, Severe Aphthous Stomatitis and Mucosal Ulcers as  
832 Primary Manifestations of a Novel STAT1 Gain-of-Function  
833 Mutation. *Front Immunol.* 2020;11:967.

834 63. Okada S, Asano T, Moriya K, Boisson-Dupuis S, Kobayashi M,  
835 Casanova JL, et al. Human STAT1 Gain-of-Function Heterozygous  
836 Mutations: Chronic Mucocutaneous Candidiasis and Type I  
837 Interferonopathy. *J Clin Immunol.* 2020;40(8):1065-81.

838 64. Neupane B, Acharya D, Nazneen F, Gonzalez-Fernandez G, Flynt  
839 AS, and Bai F. Interleukin-17A Facilitates Chikungunya Virus

840 Infection by Inhibiting IFN- $\alpha$ 2 Expression. *Front Immunol.*  
841 2020;11:588382.

842 65. Zhang J, Liu K, Zhang G, Ling N, and Chen M. Interleukin-17A  
843 pretreatment attenuates the anti-hepatitis B virus efficacy of  
844 interferon-alpha by reducing activation of the interferon-  
845 stimulated gene factor 3 transcriptional complex in hepatitis B  
846 virus-expressing HepG2 cells. *Virology Journal.* 2022;19(1):28.

847 66. Yoon CH, Kim SY, Byeon SE, Jeong Y, Lee J, Kim KP, et al. p53-derived  
848 host restriction of HIV-1 replication by protein kinase R-mediated  
849 Tat phosphorylation and inactivation. *J Virol.* 2015;89(8):4262-80.

850 67. Wang X, Majumdar T, Kessler P, Ozhegov E, Zhang Y, Chattopadhyay  
851 S, et al. STING Requires the Adaptor TRIF to Trigger Innate Immune  
852 Responses to Microbial Infection. *Cell Host Microbe.*  
853 2016;20(3):329-41.

854 68. Konkel JE, and Chen W. Balancing acts: the role of TGF- $\beta$  in the  
855 mucosal immune system. *Trends Mol Med.* 2011;17(11):668-76.

856 69. Biancheri P, Giuffrida P, Docena GH, MacDonald TT, Corazza GR,  
857 and Di Sabatino A. The role of transforming growth factor (TGF)- $\beta$  in  
858 modulating the immune response and fibrogenesis in the gut.  
859 *Cytokine Growth Factor Rev.* 2014;25(1):45-55.

860 70. Heitmann L, Rani R, Dawson L, Perkins C, Yang Y, Downey J, et al.  
861 TGF- $\beta$ -responsive myeloid cells suppress type 2 immunity and  
862 emphysematous pathology after hookworm infection. *Am J Pathol.*  
863 2012;181(3):897-906.

864 71. Andersson J, Boasso A, Nilsson J, Zhang R, Shire NJ, Lindback S, et  
865 al. The prevalence of regulatory T cells in lymphoid tissue is  
866 correlated with viral load in HIV-infected patients. *J Immunol.*  
867 2005;174(6):3143-7.

868 72. Eggena MP, Barugahare B, Jones N, Okello M, Mutalya S, Kityo C, et  
869 al. Depletion of regulatory T cells in HIV infection is associated with  
870 immune activation. *J Immunol.* 2005;174(7):4407-14.

871 73. Jiang Q, Zhang L, Wang R, Jeffrey J, Washburn ML, Brouwer D, et al.  
872 FoxP3+CD4+ regulatory T cells play an important role in acute HIV-

873 1 infection in humanized Rag2<sup>-/-</sup>-gammaC<sup>-/-</sup> mice in vivo. *Blood*.  
874 2008;112(7):2858-68.

875 74. Stapleton JT, Foung S, Muerhoff AS, Bukh J, and Simmonds P. The  
876 GB viruses: a review and proposed classification of GBV-A, GBV-C  
877 (HGV), and GBV-D in genus Pegivirus within the family Flaviviridae.  
878 *J Gen Virol*. 2011;92(Pt 2):233-46.

879 75. Heringlake S, Ockenga J, Tillmann HL, Trautwein C, Meissner D,  
880 Stoll M, et al. GB virus C/hepatitis G virus infection: a favorable  
881 prognostic factor in human immunodeficiency virus-infected  
882 patients? *J Infect Dis*. 1998;177(6):1723-6.

883 76. Nunnari G, Nigro L, Palermo F, Attanasio M, Berger A, Doerr HW, et  
884 al. Slower progression of HIV-1 infection in persons with GB virus C  
885 co-infection correlates with an intact T-helper 1 cytokine profile.  
886 *Ann Intern Med*. 2003;139(1):26-30.

887 77. Tillmann HL, Heiken H, Knapik-Botor A, Heringlake S, Ockenga J,  
888 Wilber JC, et al. Infection with GB virus C and reduced mortality  
889 among HIV-infected patients. *N Engl J Med*. 2001;345(10):715-24.

890 78. Williams CF, Klinzman D, Yamashita TE, Xiang J, Polgreen PM,  
891 Rinaldo C, et al. Persistent GB virus C infection and survival in HIV-  
892 infected men. *N Engl J Med*. 2004;350(10):981-90.

893 79. Xiang J, Wünschmann S, Diekema DJ, Klinzman D, Patrick KD,  
894 George SL, et al. Effect of coinfection with GB virus C on survival  
895 among patients with HIV infection. *N Engl J Med*. 2001;345(10):707-  
896 14.

897 80. Lalle E, Sacchi A, Abbate I, Vitale A, Martini F, D'Offizi G, et al.  
898 Activation of interferon response genes and of plasmacytoid  
899 dendritic cells in HIV-1 positive subjects with GB virus C co-  
900 infection. *Int J Immunopathol Pharmacol*. 2008;21(1):161-71.

901 81. Carvalho T, Krammer F, and Iwasaki A. The first 12 months of  
902 COVID-19: a timeline of immunological insights. *Nat Rev Immunol*.  
903 2021;21(4):245-56.

904 82. Domizio JD, Gulen MF, Saidoune F, Thacker VV, Yatim A, Sharma K,  
905 et al. The cGAS-STING pathway drives type I IFN immunopathology  
906 in COVID-19. *Nature*. 2022;603(7899):145-51.

907 83. Scagnolari C, and Antonelli G. Type I interferon and HIV: Subtle  
908 balance between antiviral activity, immunopathogenesis and the  
909 microbiome. *Cytokine Growth Factor Rev.* 2018;40:19-31.

910 84. Su L. Pathogenic Role of Type I Interferons in HIV-Induced Immune  
911 Impairments in Humanized Mice. *Curr HIV/AIDS Rep.*  
912 2019;16(3):224-9.

913 85. Bhattacharai N, McLinden JH, Xiang J, Landay AL, Chivero ET, and  
914 Stapleton JT. GB virus C particles inhibit T cell activation via  
915 envelope E2 protein-mediated inhibition of TCR signaling. *J  
916 Immunol.* 2013;190(12):6351-9.

917 86. Maidana-Giret MT, Silva TM, Sauer MM, Tomiyama H, Levi JE,  
918 Bassichetto KC, et al. GB virus type C infection modulates T-cell  
919 activation independently of HIV-1 viral load. *Aids.*  
920 2009;23(17):2277-87.

921 87. Chivero ET, Bhattacharai N, McLinden JH, Xiang J, and Stapleton JT.  
922 Human Pegivirus (HPgV; formerly known as GBV-C) inhibits IL-12  
923 dependent natural killer cell function. *Virology.* 2015;485:116-27.

924 88. Kioko M, Pance A, Mwangi S, Goulding D, Kemp A, Rono M, et al.  
925 Extracellular vesicles could be a putative posttranscriptional  
926 regulatory mechanism that shapes intracellular RNA levels in  
927 *Plasmodium falciparum.* *Nature Communications.*  
928 2023;14(1):6447.

929 89. Rieckmann JC, Geiger R, Hornburg D, Wolf T, Kveler K, Jarrossay D,  
930 et al. Social network architecture of human immune cells unveiled  
931 by quantitative proteomics. *Nat Immunol.* 2017;18(5):583-93.

932 90. Febbo PG, Mulligan MG, Slonina DA, Stegmaier K, Di Vizio D,  
933 Martinez PR, et al. Literature Lab: a method of automated literature  
934 interrogation to infer biology from microarray analysis. *BMC  
935 Genomics.* 2007;8:461.

936 91. Agrawal A, Balcı H, Hanspers K, Coort SL, Martens M, Slenter DN,  
937 et al. WikiPathways 2024: next generation pathway database.  
938 *Nucleic Acids Res.* 2024;52(D1):D679-d89.

939